Novel Spiro-Derivatives of 1,3-Thiazine Molecular Crystals: Structural and Thermodynamic Aspects

ARTICLE *in* CRYSTAL GROWTH & DESIGN · JANUARY 2013

Impact Factor: 4.89 · DOI: 10.1021/cg301511x

5 AUTHORS, INCLUDING:

German L Perlovich
Institute of Solution Chemistry of RAS
142 PUBLICATIONS **1,479** CITATIONS
SEE PROFILE

A. N. Proshin
Russian Academy of Sciences
80 PUBLICATIONS **245** CITATIONS
SEE PROFILE

CRYSTAL GROWTH & DESIGN

Article

pubs.acs.org/crystal

Novel Spiro-Derivatives of 1,3-Thiazine Molecular Crystals: Structural and Thermodynamic Aspects

German L. Perlovich,*[†,‡] Alexey N. Proshin,[‡] Marina V. Ol'khovich,[†] Angelica V. Sharapova,[†] and Anatoly S. Lermontov[§]

[†]Krestov's Institute of Solution Chemistry, Russian Academy of Sciences, 153045 Ivanovo, Russia

[‡]Institute of Physiologically Active Compounds, Russian Academy of Sciences, 142432 Chernogolovka, Russia

[§]Kurnakov's Institute of General and Inorganic Chemistry, Russian Academy of Sciences, 119991 Moscow, Russia

Supporting Information

ABSTRACT: Crystal structures of 10 spiro-derivatives of 1,3-thiazine were determined by X-ray diffraction technique. Molecular conformational states, packing architecture, and hydrogen bond networks were studied using graph set notations. Selected compounds were grouped within two classes with chains and dimer crystal structure organization. The sublimation thermodynamic aspects of the spiro-derivatives of 1,3-thiazine were investigated via temperature dependence of vapor pressure using the transpiration method. Thermophysical study of fusion processes of the molecular crystals was carried out and relationships between thermodynamic characteristics of sublimation (fusion) processes and crystal structure parameters were obtained. The influence of various molecular fragments on packing crystal energy was analyzed.

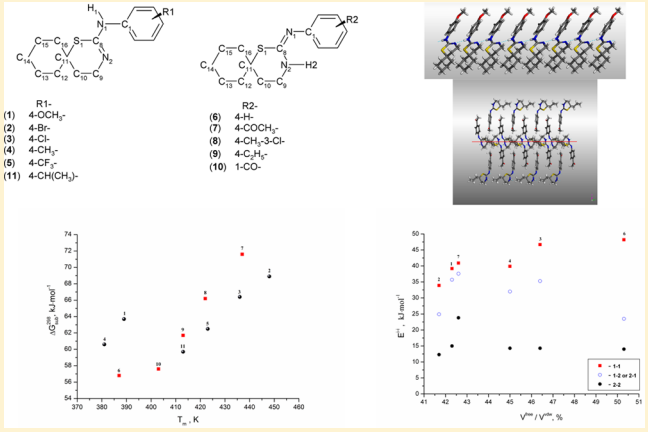

INTRODUCTION

Creation of agents blocking glutamate-induced Ca^{2+} trapping as potential neuroprotectors became one of the promising ways of developing novel drugs for the treatment of Alzheimer's and related neurodegenerative diseases.[1] As it was shown in previous work,[2] isothiourea derivatives possess neuroprotecting and cognitive-stimulating properties.

Because of the oral application of most drug compounds, the problem of their solubility requires prime attention. Solubility is a very important property of drug substances which determines both the optimal therapeutic doses and probable side effects.[3] It is interesting to note that the analysis of drug compound up-to-date databases shows that biological activity properties and solubility values are inversely proportional.[4] In other words, the substances exhibiting high affinity to the receptors have very low solubility in aqueous solutions. Therefore, it is important to create well soluble forms in order to strengthen drug compounds' position on the market.[5] There are a number of approaches to producing such forms. Most promising approaches include obtaining different polymorphic and solvatomorphic modifications,[6] particularly cocrystals and crystallosolvates/crystallohydrates.[7,8] Besides the application significance, a polymorphism comprehensive study is also important fundamentally, as it makes possible revealing the ratio between the molecular conformational flexibility and the number of potential polymorphic forms. It is also important that the molecule conformational flexibility is not a sufficient condition for polymorph formation, as in many cases nucleation and new phase growth processes are determined by the behavior of the molecular ensemble (both solute and solvent molecules), as well as by the kinetics of solvation shells rebuilding and defects relaxation in newly created crystals. However, one of the traditional ways of solubility improvement is still a structural modification of molecules.

From thermodynamics, solubility values are determined by sublimation characteristics of solids and solvation/hydration parameters of drug molecules.[9] Thermodynamic functions of molecular crystals are, in turn, directly dependent on their crystal structure. Attempts to find out the correlation between crystal structure of compounds and their thermodynamic parameters still remain a hot topic in drug/material design.

In this paper we present the results of crystal structures study, sublimation thermodynamics, and thermophysical characteristics of fusion processes, using spiro-derivatives of isothiourea (Figure 1) as an example. It should be emphasized that these compounds are interesting both fundamentally and in terms of their application as a big spiro- motive has a

Received: October 16, 2012
Revised: December 20, 2012

   dx.doi.org/10.1021/cg301511x | *Cryst. Growth Des.* XXXX, XXX, XXX−XXX

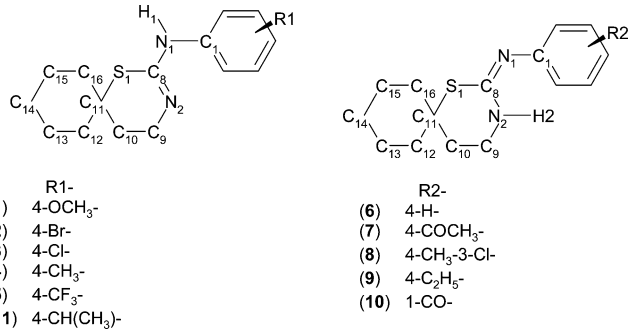

Figure 1. Structures of studied compounds with numbering of atoms.

considerable influence on crystal packing architecture and thermodynamic properties.

EXPERIMENTAL SECTION

Compounds. *Synthesis.* The following compounds were selected for the present study (Figure 1): (4-methoxy-phenyl)-(1-thia-3-aza-spiro[5.5]undec-2-en-2-yl)-amine (**1**), (4-bromo-phenyl)-1-thia-3-aza-piro[5.5]undec-2-en-2-yl)-amine (**2**), (4-chloro-phenyl)-(1-thia-3-aza-piro[5.5]undec-2-en-2-yl)-amine (**3**), (4-methyl-phenyl)-(1-thia-3-aza-spiro[5.5]undec-2-en-2-yl)-amine (**4**), (4-trifluoromethyl-phenyl)-(1-thia-3-aza-spiro[5.5]undec-2-en-2-yl)-amine (**5**), phenyl-(1-thia-3-aza-spiro[5.5]undec-2-en-2-yl)-amine (**6**), (4-acetyl-phenyl)-(1-thia-3-aza-spiro[5.5]undec-2-en-2-yl)-amine (**7**), (3-chloro-4-methyl-phenyl)-(1-thia-3-aza-spiro[5.5]undec-2-en-2-yl)-amine (**8**), (4-ethyl-phenyl)-(1-thia-3-aza-spiro[5.5]undec-2-en-2-yl)-amine (**9**), *N*-(1-thia-3-aza-spiro[5.5]undec-2-en-2-yl)-benzamide (**10**), (4-isopropyl-phenyl)-(1-thia-3-aza-spiro[5.5]undec-2-en-2-yl)-amine (**11**).

These substances have been synthesized by the reaction of an appropriate isothiocyanate with 2-cyclohex-2-enyl-ethylamine followed by cyclization of the intermediate thiourea under acidic conditions in the final bicyclic product. The chemical synthesis of compounds and confirmation of structure and purity have been described in a previous paper.[10]

Single Crystal Preparation. Single crystals of the compounds **1**−**10** were grown by slow evaporation of solvent from the toluene solution. Unfortunately, it was not possible to carry out X-ray diffraction experiments for substance **11** due to the bad quality of single crystals.

Methods. *X-ray Diffraction Experiments.* Single-crystal X-ray measurements were made using a Nonius CAD-4 diffractometer with graphite-monochromated Mo K_α radiation (λ = 0.71069 Å). Intensity data were collected at 120 K by means of a ω-2θ scanning procedure. The crystal structures were solved using direct methods and refined by means of a full-matrix least-squares procedure. CAD-4[11] was applied for data collection, data reduction and cell refinement. Programs SHELXS-97 and SHELXL-97[12] were used to solve and to refine structures, respectively.

Sublimation Experiments. Sublimation experiments were carried out by the transpiration method as was described elsewhere.[13] In brief: a stream of an inert gas passes above the sample at a constant temperature and at a known slow constant flow rate in order to achieve saturation of the carrier gas with the vapor of the substance under investigation. The vapor is condensed at some point downstream, and the mass of sublimate and its purity are determined. The vapor pressure over the sample at this temperature can be calculated by the amount of the sublimated sample and the volume of the inert gas used.

The equipment was calibrated using benzoic acid. The standard value of sublimation enthalpy obtained here was ΔH^0_{sub} = 90.5 ± 0.3 kJ·mol^{-1}. This is in good agreement with the value recommended by IUPAC of ΔH^0_{sub} = 89.7 ± 0.5 kJ·mol^{-1}.[14] The saturated vapor pressures were measured five times at each temperature with the standard deviation being within 3−5%. Because the saturated vapor pressure of the investigated compounds is low, it may be assumed that the heat capacity change of the vapor with temperature is so small that it can be neglected. The experimentally determined vapor pressure data may be described in (ln P; 1/T) coordinates in the following way:

$$\ln P = A + B/T \quad (1)$$

The value of the sublimation enthalpy is calculated by the Clausius−Clapeyron equation:

$$\Delta H^T_{sub} = RT^2 \cdot \partial(\ln P)/\partial(T) \quad (2)$$

whereas the sublimation entropy at the given temperature T was calculated from the following relation:

$$\Delta S^T_{sub} = (\Delta H^T_{sub} - \Delta G^T_{sub})/T \quad (3)$$

with $\Delta G^T_{sub} = -RT \ln(P/P_0)$, where P_0 is the standard pressure of 1 × 10^5 Pa.

For experimental reasons sublimation data are obtained at elevated temperatures. However, in comparison with effusion methods, the temperatures are much lower, which makes extrapolation to room conditions easier. In order to further improve the extrapolation to room conditions, we estimated the heat capacities ($C^{298}_{p,cr}$-value) of the crystals using the additive scheme proposed by Chickos et al.[15] Heat capacity was introduced as a correction for the recalculation of the sublimation enthalpy ΔH^T_{sub}-value at 298 K (ΔH^{298}_{sub}-value), according to the equation:[15]

$$\Delta H^{298}_{sub} = \Delta H^T_{sub} + \Delta H_{cor} = \Delta H^T_{sub} + (0.75 + 0.15 \cdot C^{298}_{p,cr} \cdot (T - 298.15) \quad (4)$$

Differential Scanning Calorimetry. The thermal analysis experiment was carried out by DSC 204 F1 Phoenix differential scanning heat flux calorimeter (NETZSCH, Germany) with a high sensitivity μ-sensor. A sample was heated at 10 $K \cdot min^{-1}$ in argon and cooled by gaseous nitrogen. The DSC temperature calibration was performed against six high-purity substances: cyclohexane (99.96%), mercury (99.99+%), biphenyl (99.5%), indium (99.999%), tin (99.999%), and bismuth (99.9995%). The accuracy of the weighing procedure was ±0.01 mg.

Calculation Procedure. The free molecular volume in the crystal lattice was estimated on the basis of the X-ray diffraction data and van der Waals molecular volume (V^{vdw}), calculated by GEPOL.[16] For the disordered structures V^{vdw}-values have been calculated for the coordinates of atoms with maximal probability. Molecular free volume V^{free} has been evaluated as

$$V^{free} = (V_{cell} - Z \cdot V^{vdw})/Z \quad (5)$$

where V_{cell} is the volume of the unit cell, and Z is the number of molecules in the unit cell.

Nonbonded van der Waals interactions of crystal lattice energy were calculated as a sum of atom−atom interactions with the help of Gavezzotti et al. (exponential-6 form)[17] force field with cutoff radius of 16 Å. The choice of this force field can be explained by the following reasons. First, the potential function used for the pairwise calculations was carefully calibrated and validated for the numerous molecular crystals (by comparing the calculated and experimental data for sublimation enthalpies). The sublimation characteristics of the chosen substances will be discussed by us in detail below. Second, we tried to compare the experimental values of sublimation enthalpies for different molecular crystal classes with the results of crystal lattice energy calculations in which other force fields were used (for example, Mayo et al.[30] (Lenard-Jones 12−6)). As a result, we came to a conclusion that it is by Gavezzotti's force field that the experimental values are best described. Even corrections to the Mayo force field for electrostatic interactions did not improve the values obtained by Gavezzotti's force field. The noted calculations were carried out by homemade software.

RESULTS AND DISCUSSION

Crystal Structure Analysis. The results of the X-ray diffraction experiments are presented in Table 1.

dx.doi.org/10.1021/cg301511x | Cryst. Growth Des. XXXX, XXX, XXX−XXX

Table 1. Crystal Lattice Parameters of the Substances under Investigation[a]

	1	2	3	4	5
CCDC code	894490	894492	894495	894493	894499
crystal system	monoclinic	monoclinic	monoclinic	monoclinic	triclinic
space group	$P2_1/c$	$P2_1/c$	$P2_1/c$	$P2_1/c$	$P\bar{1}$
crystal size, mm	0.12 × 0.10 × 0.09	0.19 × 0.08 × 0.03	0.5 × 0.20 × 0.19	0.10 × 0.06 × 0.02	0.10 × 0.04 × 0.02
a, Å	13.057(4)	13.000(3)	12.7995(7)	12.855(6)	13.595(5)
b, Å	14.628 (4)	15.170(3)	15.1263(9)	14.961(7)	15.382(5)
c, Å	8.306(2)	7.7773(16)	7.9069(5)	7.931(4)	7.787(3)
α, °	90	90	90	90	90
β, °	108.295(4)	104.832(3)	104.423(10)	103.716(8)	93.635(6)
γ, °	90	90	90	90	106.408(6)
volume, Å^3	1506.3(7)	1482.7(5)	1482.6(15)	1481.8(12)	1558.5(9)
Z	4	4	4	4	4
D_{calc}, g·cm^{-3}	1.281	1.520	1.321	1.230	1.400
radiation	Mo K_α	Mo K_α	Mo K_α	Mo K_α	Mo K_α
T, K	173(2)	173(2)	296(2)	173(2)	173(2)
μ, mm^{-1}	0.213	2.902	0.387	0.477	0.237
Data Collection					
measured reflections	12003	11921	12273	11030	14942
independent reflections	3277	3090	3227	2886	6780
independent reflections with >2$\sigma(I)$	2705	2511	2699	2161	4458
R_{int}	0.0384	0.0428	0.0283	0.0821	0.0633
θ_{max}, °	27.0	26.58	26.99	25.99	27.00
Refinement					
refinement on	F^2	F^2	F^2	F^2	F^2
$R[F^2 > 2\sigma(F^2)]$	0.0357	0.0280	0.0365	0.0509	0.0574
$\omega R(F^2)$	0.0890	0.064	0.0943	0.1397	0.1369
S	1.062	1.033	1.072	1.016	1.021
reflections	3277	3090	3227	2886	6780
parameters	269	176	249	177	426
$(\Delta/\sigma)_{max}$	0.000	0.001	0.001	0.001	0.000
$\Delta\rho_{max}$, e·Å^{-3}	0.30	0.341	0.453	0.334	0.657
$\Delta\rho_{min}$, e·Å^{-3}	−0.19	−0.333	−0.321	−0.330	−0.566
V^{vdw}, Å^3	264.6	261.5	253.1	255.4	264.3
V^{free}, Å^3	112.0	109.2	117.6	115.1	125.3
$\beta = V^{free}/V^{vdw}$, %	42.4	41.8	46.5	45.1	47.4
$K = V^{vdw}/V_{mol}$, %	70.3	70.5	68.3	68.9	67.8
	6	**7**	**8**	**9**	**10**
CCDC	894498	894497	894496	894494	894491
crystal system	monoclinic	monoclinic	monoclinic	orthorhombic	monoclinic
space group	$P2_1/n$	$P2_1/n$	$P2_1/c$	$Pna2_1$	$P2_1/n$
crystal size, mm	0.12 × 0.08 × 0.07	0.12 × 0.12 × 0.12	0.15 × 0.09 × 0.08	0.09 × 0.08 × 0.08	0.49 × 0.40 × 0.25
a, Å	6.235(3)	10.611(5)	13.064(3)	19.395(3)	9.6555(6)
b, Å	19.286(8)	7.779(3)	9.3997(19)	6.1309(10)	13.1733(9)
c, Å	11.982(5)	19.234(8)	13.724(3)	27.533(4)	12.7112(8)
α, °	90	90	90	90	90
β, °	96.517(7)	101.253(6)	113.821(3)	90(2)	110.134(10)
γ, °	90	90	90	90	90
volume, Å^3	1431.4(10)	1557.0(11)	1541.7(5)	3273.9(9)	1518.0(17)
Z	4	4	4	8	4
D_{calc}, g·cm^{-3}	1.208	1.290	1.331	1.170	1.262
radiation	Mo K_α	Mo K_α	Mo K_α	Mo K_α	Mo K_α
T, K	296(2)	173(2)	173(2)	296(2)	296(2)
μ, mm^{-1}	0.211	0.209	0.375	0.191	0.211
Data Collection					
measured reflections	11001	14076	12635	24684	14226
independent reflections	2800	3395	3360	3426	3317
independent reflections with >2$\sigma(I)$	1918	2582	2739	2466	2824
R_{int}	0.0407	0.0667	0.0397	0.0595	0.0232
θ_{max}, °	26.0	27.0	27.00	26.38	27
Refinement					

dx.doi.org/10.1021/cg301511x | Cryst. Growth Des. XXXX, XXX, XXX−XXX

Table 1. continued

	6	7	8	9	10
refinement on	F^2	F^2	F^2	F^2	F^2
$R[F^2 > 2\sigma(F^2)]$	0.0609	0.0534	0.0356	0.0464	0.0365
$\omega R(F^2)$	0.1650	0.1366	0.0846	0.1222	0.0976
S	1.018	1.021	1.044	1.032	1.067
reflections	2800	3395	3360	3426	3317
parameters	166	195	186	366	261
$(\Delta/\sigma)_{max}$	0.000	0.000	0.001	0.000	0.001
$\Delta\rho_{max}$, e·Å^{-3}	0.59	0.54	0.273	0.386	0.188
$\Delta\rho_{min}$, e·Å^{-3}	−0.31	−0.40	−0.211	−0.233	−0.223
V^{vdw}, Å^3	238.0	273.0	270.1	268.4	257.2
V^{free}, Å^3	119.8	116.2	115.3	140.8	122.3
$\beta = V^{free}/V^{vdw}$, %	50.3	42.6	42.7	52.5	47.6
$K = V^{vdw}/V_{mol}$, %	66.5	70.1	70.1	65.6	67.8

[a]Standard deviations are presented in brackets.

Table 2. Hydrogen Bond Geometry and Graph Set Notations of the Molecules Studied

compound	D—H···A	D—H [Å]	H···A [Å]	D···A [Å]	D—H···A [deg]	symmetry code	
1	N1—H1···N2	0.85(2)	2.13(2)	2.98(2)	175(2)	$x, -y + 1/2, z - 1/2$	$C_1^1(4)$
2	N1—H1···N2	0.79(3)	2.15(3)	2.93(3)	176(3)	$x, -y + 1/2, z + 1/2$	$C_1^1(4)$
3	N1—H1···N2	0.83(3)	2.13(3)	2.96(3)	176(2)	$x, -y + 1/2, z - 1/2$	$C_1^1(4)$
4	N1—H1···N2	0.84(3)	2.11(3)	2.95(3)	174(2)	$x, -y + 1/2, z - 1/2$	$C_1^1(4)$
5	N1—H1···N2	0.89(3)	2.05(3)	2.93(3)	174(3)	$-x + 2, -y + 2, -z$	$C_1^1(4)$
6	N1···H2—N2	0.84(2)	2.12(2)	2.96(4)	175(3)	$-x + 1, -y, z + 2$	$R_2^2(8)$
7	N1···H2—N2	0.82(3)	2.11(3)	2.93(3)	177(2)	$-x, -y + 1, -z$	$R_2^2(8)$
8	N1···H2—N2	0.84(2)	2.09(2)	2.92(2)	172(2)	$-x + 2, -y + 2, -z + 1$	$R_2^2(8)$
9	N1···H2—N2	0.81(3)	2.16(3)	2.97(3)	176(2)		$R_2^2(8)$
10	N2—H2···O1	0.86(2)	3.32(3)	2.46(3)	133(3)	$-x, -y, -z + 2$	$R_2^2(12)$
10	N2—H2···O1	0.86(2)	1.99(3)	2.65(3)	133(3)		S(6)

Packing Architecture Analysis. Hydrogen bonds geometry of the studied compounds is given in Table 2.

In terms of hydrogen bond network topology, all compounds can be conventionally subdivided into two groups. The first one contains the compounds that form infinite chains of hydrogen bonds with four included atoms, $C_1^1(4)$, (**1**−**5**), while the second one contains dimers forming rings with eight atoms, $R_2^2(8)$, (**6**−**10**). Hydrogen bond topology network (strength and three-dimensional structure) contributes to thermodynamic parameters of a crystal. Having solved crystal structures and thermodynamic characteristics of sublimation and fusion processes, we tried to identify some regularities in the behavior of the properties involved. Before starting this analysis, we would like to specify molecular packing of the crystals of each group.

Compounds with hydrogen bond networks $C_1^1(4)$ form chains oriented along the *c*-axis for compounds **1**−**5**. As an example, two perpendicular projections of the discussed chains are shown in Figure 2 for compound **2** (the rest of the substances have analogous projections).

The structures **1**−**5** are essentially "isostructural". For structures **2**−**4**, an interchange of the Me-, Cl-, or Br-substituents has essentially no effect at all on the crystal structure (apart from the very minor metric differences visible in Table 1), while the methoxy group in **1** has a slightly greater influence. The structures are best described as having layers in the *bc* planes. The small difference for **1** compared to **2**−**4** is most clearly visible in the beta angle (108 vs 104 deg), which reflects the fact that adjacent layers are offset slightly compared to their position in **2**−**4** (Figure 3a). Structure **5** contains identical layers, but it has a different relative arrangement of layers; in other words, structure **5** is essentially a "polytype" of structures **1**−**4** (Figure 3b).

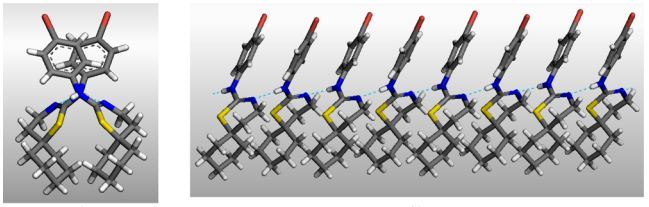

Figure 2. A view of molecular chain along the two axes for the compound with chain organization of the crystal structure (**2**): (a) along *c*, (b) along *b*.

Analysis of molecular packing projection along the *c*-axis (Figure 4) makes it possible to reveal the following regularities. The whole space is packed with two-dimensional chains oriented in the *c*-direction (as an example of similar molecular packing of the structures **1**−**4**, projection **2** is presented in Figure 4a). One of the borders of the chain periphery consists of spiro- fragments, while the other one consists of phenyl-derivative motives. Each chain comes in contact with a neighboring (adjacent) one along the borders (spiro- -phenyl-fragments). Thus, the chains interact through van der Waals forces only (nonspecific interactions). However, the packing of chains in compound **5** slightly differs from the rest of the compounds in this group. It may be explained by the fact that fluoromethyl- and spiro- fragments come in contact with comparable fragments of adjacent molecules (see indications in

dx.doi.org/10.1021/cg301511x | *Cryst. Growth Des.* XXXX, XXX, XXX−XXX

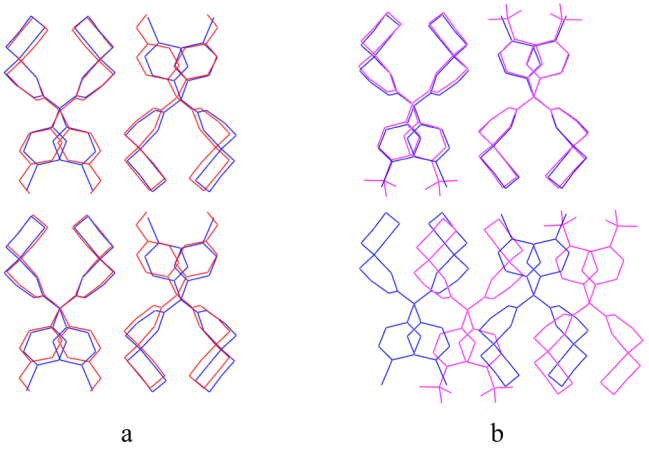

Figure 3. Comparative molecular packing projections along the *c*-axis for the compounds studied: (a) (**1** - red) and (**2** - blue); (b) (**5** - pink) and (**2** - blue).

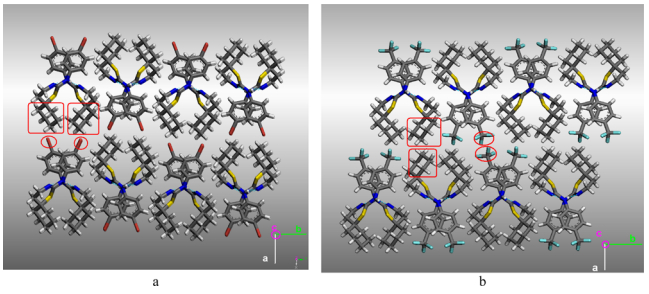

Figure 4. Molecular packing projections for the compounds studied along the *c*-axis: (a) (**2**); (b) (**5**).

Figure 4b). No comparable contacts in adjacent molecules of other compounds are observed.

Compounds with dimer crystal packing architecture (**6**–**9**) may be described in the following way. Molecules form dimers having a hydrogen bond network described by a topological graph $R_2^2(8)$. Different dimer projections are shown in Figure 1 Supporting Information. The specific way of dimers packing in the crystals is responsible for unique behavior of thermodynamic functions of sublimation and fusion processes. For example, dimers of compound **6** are packed in columns. Each dimer in the column is in parallel to that above or below it (Figure 5a, red color). Dimer columns interact at the expense of weak van der Waals forces and thus form a crystal (Figure 5b, red ellipse). Therefore, molecule packing of the crystal

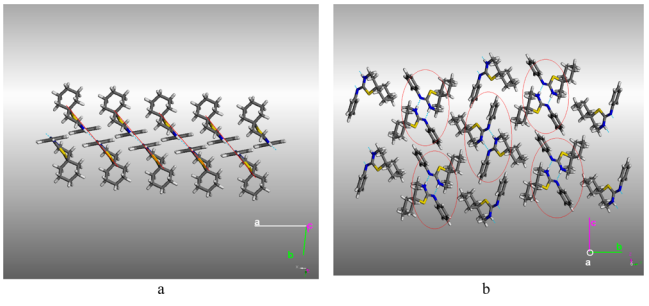

Figure 5. Two perpendicular projections of molecular packing (**6**) with dimer organization of crystal structure (red lines correspond to planes of the dimers (a); red ellipses correspond to columns of the dimers (b)).

bears resemblance to a chain structure; i.e., here and there molecules form chains at the expense of $C_1^1(4)$ graph in one case, and at the expense of interaction between adjacent dimers in the other case.

Dimers of compound **7** are packed in a similar way, that is, in the form of columns oriented along the *b*-axis. In the column dimers are parallel to each other (Figure 6: the direction of the

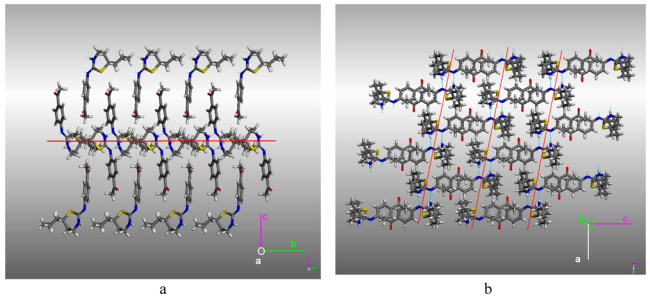

Figure 6. Two perpendicular projections of molecular packing (**7**) with dimer organization of crystal structure (red lines on a and b correspond to orientation of the dimer columns).

packed molecules in a column is defined by the red line). Specific feature of column packing in a crystal of the compound discussed is that adjacent columns interact through 4-$COCH_3$-Ph fragments that are packed in piles, with each adjacent fragment belonging to different dimer columns (dimer column interaction looks like "overlapping fingers").

Molecular packing of compound **9** is presented in Figure 2 Supporting Information which is like one in compound **6**. Molecular packing of crystal **8** differs considerably from the noted dimer structures. It is evidently connected with the presence of two substituents in the phenyl ring. Molecules form dimers. The planes of adjacent dimers are at an angle of 67° to each other (Figure 7a: lines correspond to dimer planes). The conditional planes, where the dimers are situated, form a parallelepiped. The whole crystal is packed in this way (Figure 7b).

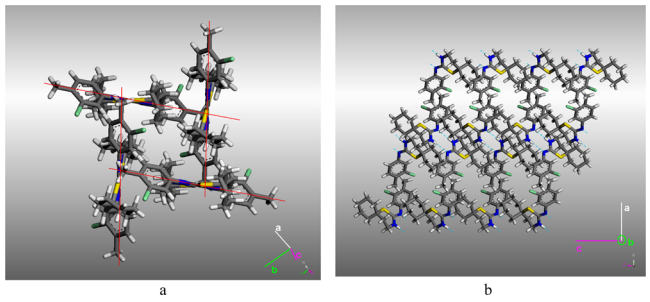

Figure 7. Two projections of molecular packing (**8**) with dimer organization of crystal structure (red lines on a) correspond to planes of the dimers).

Like all the compounds of the second group, compound **10** also forms dimers. These, in turn, form zigzag-like surfaces when every adjacent surface is formed by dimers with deployed planes (Figure 8a,b). In this figure dimer planes with different orientation are indicated by different colors letters. Zigzag-like surfaces interact only through van der Waals forces.

Molecular Conformational Analysis. Conformational state of a molecule is defined by both steric hindrances and its packing in a crystal. That is why we attempted to analyze the

dx.doi.org/10.1021/cg301511x | *Cryst. Growth Des.* XXXX, XXX, XXX–XXX

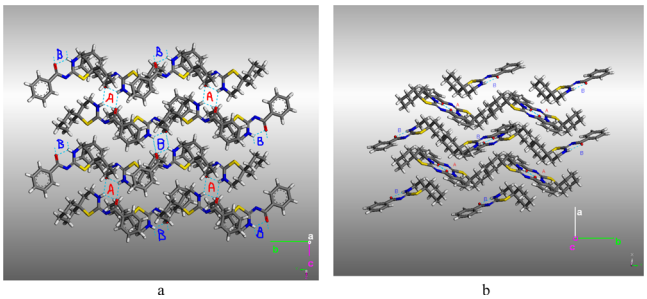

a b

Figure 8. Two projections of molecular packing (**10**) with dimer organization of crystal structure (letters A and B corresponds to dimers with different orientation).

mentioned problems and find out regularities that can cause changes in parameters describing the conformational molecule state. To describe molecular conformations we selected the angles presented in Table 3 (numbering corresponds to that presented in Figure 1).

To bring all conformations into a comparable form, the molecules with positive ∠N2−C8−N1−C1 angles in the unit cells have been analyzed. Hence, all the compounds have been arbitrarily subdivided into two groups. The first group contains molecules that form dimers with hydrogen bond network $R_2^2(8)$ and the angles close to 180° (**6**−**9**). The second group consists of compounds forming infinite chains with four included atoms ($C_1^1(4)$) and small angle values (**1**−**5**).

Each cycle of spiro- fragments of the compounds studied is considerably deformed. Therefore, to describe these deformations, the following dihedral angles have been introduced ∠C11−C10−C9−N2 and ∠C11−S1−C8−N2 for 1,3-thiazine fragment, as well as ∠C11−C16−C15−C14 and ∠C11−C12−C13−C14 for cyclohexane fragment. In order to characterize molecular packing of a crystal it has been selected parameter $\beta = V^{free}/V^{vdw}$. Angle values ∠C11−C10−C9−N2 for all compounds concerned do not vary a lot (their values are in the range from −65° to −50°); except for compounds **7** and **8** that have positive values (Figure 3 Supporting Information). If we analyze dihedral angles ∠C9−C10−C11−C16 as a function of β-parameter (Figure 9), we will see that the angle remains unchanged for compounds with hydrogen bond networks in the form of infinite chains ($C_1^1(4)$). For the compounds forming dimers ($R_2^2(8)$), the angle grows with diminishing molecular packing density in a crystal (increasing β-parameter). The cyclohexane fragment is configured as a "chair" conformation for all compounds. A small difference is observed between ∠C11−C16−C15−C14 and ∠C11−C12 −C13−C14

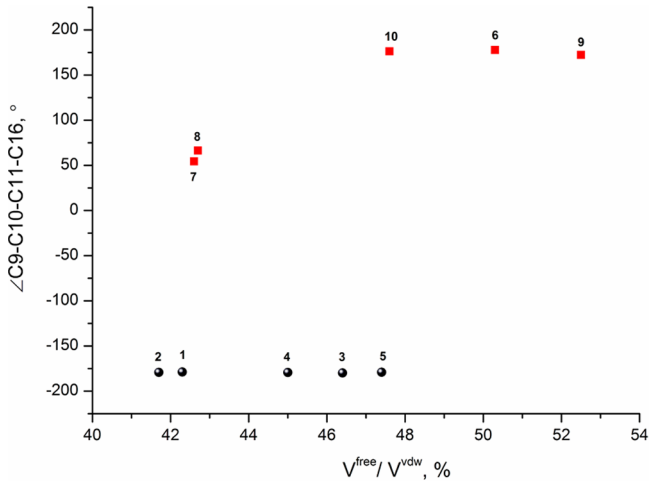

Figure 9. Plot of ∠C9−C10−C11−C16 versus V^{free}/V^{vdw} for the compounds studied (red squares correspond to the crystals with dimers organization, black circles − with chains organization). Numbering corresponds to Figure 1.

values for various substances, while for compound **7** they differ greatly and have the opposite sign.

Sublimation and Fusion Characteristics. The temperature dependencies of saturated vapor pressure of **1**−**11** are shown in Table 4. The thermodynamic functions of the drugs sublimation and fusion processes are presented in Table 5.

Relationship between Thermodynamic Characteristics and Crystal Structure. The search for regularities between thermodynamic (sublimation), thermophysical (fusion process) characteristics and crystal structure parameters has always been one of the main problems highlighted in the literature.[18−22] Long ago Kitaigorodsky[23] suggested that various physicochemical properties should be correlated with a parameter describing molecular packing density in a crystal (V^{vdw}/V^{mol}). We have modified this parameter[22,24−26] ($\beta = V^{free}/V^{vdw}$) to attract attention to the free volume (V^{free}) which the molecule has in a crystal. In general, V^{free} is an integrate (composite) value that comprises: (a) free volume configured as a result of complex topological structure and steric hindrances of conformationally flexible molecules in a crystal (the so-called free volume, which is determined due to the structure of a molecule in a conformational state it has in a crystal); (b) free volume as a result of molecular packing in a crystal (corresponding to equilibrium crystal defects). It is difficult to separate the first part of V^{free} from the other, as they perform different functions in the processes occurring in

Table 3. Some Parameters (in °) Describing Molecular Conformation in the Crystals

compound	∠N2−C8 −N1−C1	∠C11−C10 −C9−N2	∠C11−S1− C8−N2	∠C11−C16 −C15−C14	∠C11−C12 −C13−C14	∠C9−C10 −C11−C12	∠C9−C10 −C11−C16	∠C8−S1 −C11−C16
1	5.0	−51.8	12.8	53.7	−55.5	−55.8	−178.8	−160.5
2	13.7	−52.0	12.9	52.5	−56.2	−56.3	−179.2	−159.8
3	13.2	−52.6	12.2	52.5	−56.0	−56.9	−179.9	−159.1
4	14.0	−52.0	12.2	52.8	−55.8	−56.3	−179.4	−159.8
5	17.6	−49.2	13.8	53.9	−55.5	−56.0	−179.1	−159.7
6	177	−56.9	7.7	53.6	−47.6	−58.1	177.8	−152.8
7	179.6	48.1	−14.0	−55.0	57.4	178.8	54.5	−77.1
8	179.9	66.1	12.1	55.8	−54.6	−171.1	66.5	−105.9
9	175.5	−65.0	4.8	54.3	−56.4	−66.2	172.4	−144.4
10	0.4	−61.8	0.9	50.9	−56.9	−60.3	176.3	−148.3

dx.doi.org/10.1021/cg301511x | Cryst. Growth Des. XXXX, XXX, XXX−XXX

Table 4. Temperature Dependencies of Saturation Vapor Pressure of the Compounds Studied[a]

1[b]		2		3		4		5		6		7	
T	$P{\cdot}10^3$	T	$P{\cdot}10^3$	T	$P{\cdot}10^2$	T	$P{\cdot}10^3$	T	$P{\cdot}10^2$	T	$P{\cdot}10^3$	T	$P{\cdot}10^2$
80.0	3.35	101.0	5.7	97.0	1.08	80.0	9.40	111.5	4.95	69.0	6.90	112.0	1.87
82.0	4.65	102.0	7.6	99.0	1.28	82.0	12.9	112.4	5.32	70.0	8.20	113.0	2.16
85.0	6.55	105.0	10.5	100.0	1.29	84.0	15.8	112.8	5.53	73.0	10.1	114.0	2.52
87.0	9.47	107.0	13.5	103.0	1.99	87.0	22.4	113.8	6.20	74.0	13.2	115.0	2.86
89.0	11.5	112.0	19.2	105.0	2.79	90.0	30.2	115.6	7.35	76.0	14.7	117.0	3.43
92.0	16.4	115.0	32.0	107.0	3.58	92.0	36.6	116.9	8.50	77.0	18.0	118.0	3.74
94.0	21.7	118.0	41.7	110.0	5.41	94.0	45.4	118.1	9.41	79.0	23.9	119.0	4.45
96.0	27.3	120.0	55.0	112.0	7.05	96.0	67.3	119.7	10.7	82.0	31.4	120.0	5.04
98.0	36.3	122.0	67.4	114.0	7.69	99.0	97.6	120.7	11.9	84.0	44.2	121.0	5.59
100.0	42.8	124.0	79.9	116.0	8.96	102.0	138	122.1	13.7	87.0	62.2	123.0	7.29
102.0	52.3	126.0	95.0	118.0	11.7	103.0	137	123.6	15.0	88.0	63.4	124.0	7.99
104.0	66.3	128.0	124	120.0	14.9	104.0	155	125.1	18.8	90.0	91.0	125.0	9.17
108.0	97.3	130.0	145	122.0	18.6	105.0	185	126.5	22.2	92.0	104	127.0	11.1
		132.0	181	124.0	21.8	107.0	234	127.9	22.4	94.0	130	128.0	12.2
		134.0	215	127.0	28.0	111.0	351	129.2	27.6	95.0	135	129.0	14.4
		136.0	277	130.0	39.0			130.4	28.6	96.0	154	131.0	17.2
		138.0	348										

8[c]		9		10		11	
T	$P{\cdot}10^3$	T	$P{\cdot}10^2$	T	$P{\cdot}10^3$	T	$P{\cdot}10^2$
112.0	7.9	93.0	3.45	80.0	2.18	92.0	1.98
113.0	8.8	95.0	4.16	81.0	2.34	93.0	2.34
114.0	11.3	97.5	5.31	84.0	3.09	96.0	3.21
116.0	12.2	99.5	70.8	87.0	3.78	98.0	3.70
117.0	12.9	101.0	8.22	90.0	4.76	100.0	4.74
118.0	15.9	103.0	11.5	93.0	5.80	102.0	5.94
120.0	17.9	105.0	14.3	95.0	6.82	104.0	7.14
122.0	20.5	107.0	15.8	98.0	8.90	106.0	8.30
123.0	22.9	109.0	21.3	100.0	10.6	108.0	10.5
125.0	29.5	111.0	25.7	102.0	12.8	110.0	12.5
127.0	33.1	113.0	32.7	104.0	14.0	112.0	15.3
128.0	34.0	115.0	36.3	105.0	15.1	114.0	19.3
129.0	37.5	117.0	46.3	107.0	18.5	115.0	19.9
131.0	45.5	119.0	64.2	108.0	20.0	118.0	26.0
132.0	50.9	121.0	79.8	110.0	22.6	120.0	33.6
133.0	53.4			113.0	28.7		
135.0	60.9						

[a]Units: T in °C; P in Pa. [b](**1**) $\ln(P[\text{Pa}]) = (40.3 \pm 0.6) - (16236 \pm 231)/T$; (**2**) $\ln(P[\text{Pa}]) = (38.9 \pm 0.5) - (16463 \pm 196)/T$; (**3**) $\ln(P[\text{Pa}]) = (40.1 \pm 0.4) - (16512 \pm 175)/T$; (**4**) $\ln(P[\text{Pa}]) = (40.2 \pm 0.6) - (15834 \pm 230)/T$; (**5**) $\ln(P[\text{Pa}]) = (35.3 \pm 0.4) - (14746 \pm 176)/T$; (**6**) $\ln(P[\text{Pa}]) = (38.3 \pm 0.6) - (14821 \pm 226)/T$; (**7**) $\ln(P[\text{Pa}]) = (31.5 \pm 0.4) - (12866 \pm 162)/T$. [c](**8**) $\ln(P[\text{Pa}]) = (31.0 \pm 0.6) - (13767 \pm 224)/T$; (**9**) $\ln(P[\text{Pa}]) = (40.6 \pm 0.6) - (16098 \pm 225)/T$; (**10**) $\ln(P[\text{Pa}]) = (23.9 \pm 0.3) - (10623 \pm 110)/T$; (**11**) $\ln(P[\text{Pa}]) = (34.9 \pm 0.3) - (14164 \pm 128)/T$.

Table 5. Thermodynamic Characteristics of Sublimation and Fusion Processes of the Compounds Studied

compound	$\Delta G^{298}_{\text{sub}}$, [kJ·mol^{-1}]	Δ^{T}_{sub}, [kJ·mol^{-1}]	$C^{298a}_{p_c}$, [J·mol^{-1}·K^{-1}]	$\Delta H^{298b}_{\text{sub}}$, [kJ·mol^{-1}]	$T\Delta S^{298}_{\text{sub}}$, [kJ·mol^{-1}]	$\Delta S^{298}_{\text{sub}}$, [J·mol^{-1}·K^{-1}]	T_m, [K]	$\Delta H^{T}_{\text{fus}}$, [kJ·mol^{-1}]	$\Delta S^{T}_{\text{fus}}$, [J·mol^{-1}·K^{-1}]
1	63.7 ± 0.8	135.0 ± 1.9	394.1	139.1 ± 1.9	69.0 ± 1.2	253 ± 5	388.4 ± 0.2	29.3 ± 0.5	75.4 ± 1.3
2	68.9 ± 0.8	136.8 ± 1.6	340.1	141.6 ± 1.6	72.7 ± 2.2	244 ± 7	448.3 ± 0.2	44.3 ± 0.5	98.8 ± 1.1
3	66.4 ± 0.7	137.3 ± 1.4	336.4	141.7 ± 1.4	75.3 ± 2.2	253 ± 8	435.7 ± 0.2	41.9 ± 0.5	96.2 ± 1.1
4	60.6 ± 0.6	131.6 ± 1.9	344.3	136.8 ± 1.9	76.2 ± 2.6	256 ± 9	381.3 ± 0.2	29.7 ± 0.5	73.8 ± 1.2
5	62.5 ± 0.7	122.6 ± 1.4	409.5	128.5 ± 1.4	66.0 ± 1.3	221 ± 4	422.8 ± 0.2	32.9 ± 0.5	77.8 ± 1.2
6	56.8 ± 1.9	123.2 ± 1.9	307.7	125.9 ± 1.9	69.1 ± 1.6	232 ± 5	386.5 ± 0.2	21.6 ± 0.5	55.8 ± 1.3
7	71.6 ± 1.2	151.6 ± 1.4	372.3	156.0 ± 1.4	84.4 ± 2.4	283 ± 8	436.5 ± 0.2	32.5 ± 0.5	74.4 ± 1.1
8	66.2 ± 0.9	114.5 ± 1.8	373.0	120.1 ± 1.8	53.9 ± 1.7	181 ± 5	422.3 ± 0.2	33.2 ± 0.5	78.6 ± 1.2
9	61.7 ± 1.8	138.3 ± 1.8	371.2	138.3 ± 1.8	76.6 ± 2.5	257 ± 8	412.5 ± 0.2	42.8 ± 0.5	40.5 ± 0.5
10	57.6 ± 0.6	88.3 ± 0.9	344.7	92.0 ± 0.9	31.4 ± 0.9	115 ± 3	403.3 ± 0.2	27.9 ± 0.5	69.2 ± 0.8
11	59.7 ± 0.6	117.8 ± 1.1	408.2	122.8 ± 1.1	63.1 ± 1.8	212 ± 6	412.7 ± 0.2	29.2 ± 0.5	70.8 ± 1.2

[a]$C^{298}_{p_c}$ was estimated using the additive scheme proposed by Chickos et al.[15] [b]$\Delta H^{298}_{\text{sub}} = \Delta H^{T}_{\text{sub}} + [0.75 + 0.15 \cdot C^{\text{crystal}}_{p}(298.15)]\cdot(T - 298.15)$.[15]

dx.doi.org/10.1021/cg301511x | Cryst. Growth Des. XXXX, XXX, XXX−XXX

crystals during sublimation and fusion. For example, such defects as vacancies (in other words − free volume) are responsible for "stepped mechanism" of molecular crystal sublimation.[27] As a result, we analyzed thermodynamic parameters as a function of V^{free}. Examining the molecule topology effect on crystal packing architecture and thermodynamic characteristics respectively requires β-parameter analysis (or D_{calc}). This approach can be explained by the fact that there is a considerable change in molecular conformation state during crystal lattice shaping. As a consequence, a nonadditive increase in free volume per molecule in a crystal is observed due to the gain in van der Waals volume. If we want to study only the influence of the molecular size on the above processes, it would be better to use V^{vdw}. Analysis of experimental values β versus V^{vdw} (Figure 10) makes it possible to describe how much the molecular topology influences the packing characteristics in a crystal. Compounds with dimer organization of crystal structure are indicated by red dots. It is evident that compounds with approximately equal van der Waals volumes possess quite different packing density values of packing (4-C_2H_5−Ph- - **9** and 4-CH_3-3-Cl-Ph- - **8**; 4-CF_3−Ph- - **5** and 4-OCH_3−Ph- - **1**). It is interesting to note that introducing any substituent in the para- position of phenyl ring increases molecular packing density in a crystal (the decrease in β). In the case with 4-C_2H_5−Ph- substituent (**9**), molecular packing density diminishes strongly as compared to unsubstituted compound. The crystal structure of compound **9** adopts the non-centrosymmetric space group $Pna2_1$, but it contains dimers that are clearly centrosymmetric. It is just interesting and worth mentioning that these centers of symmetry are "pseudosymmetry elements". Hence, in our opinion, it would be reasonable to analyze thermodynamic functions of compounds using both β and V^{vdw} parameters.

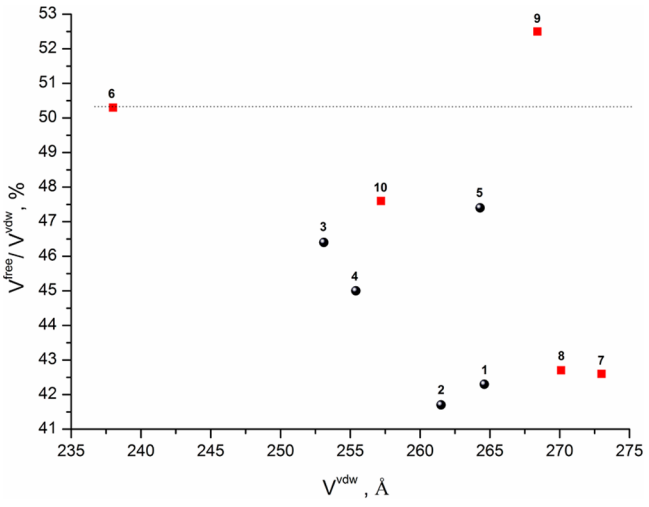

Figure 10. Plot of V^{free}/V^{vdw} versus V^{vdw} for the compounds studied (red squares correspond to the crystals with dimers organization, black circles − with chains organization). Numbering corresponds to Figure 1.

The experimental values of ΔG^{298}_{sub} as functions of β (a) and V^{vdw} (b) are presented in Figure 11a,b, respectively. Analysis of compounds with dimer organization of crystal structure (red dots) shows that the decrease in Gibbs energy of sublimation is accompanied by the increase of β-parameter, the exception being values for 4-C_2H_5−Ph- derivatives (**9**). ΔG^{298}_{sub}-value increases in V^{vdw} coordinates with the proliferation of van der Waals volume. If we study compounds with a chain-like structure (black dots), it is not difficult to see that they fall into two groups in β and V^{vdw} coordinates. Experimental dots of different groups do not fall into the same coordinate system. For example, the first group in β coordinates includes 4-Br-Ph- (**2**); 4-Cl-Ph- (**3**); 4-CF_3−Ph- (**5**), while the second one has 4-OCH_3−Ph- (**1**); 4-CH_3−Ph- (**4**). The first group in V^{vdw} coordinates includes 4-Br-Ph- (**2**); 4-Cl-Ph- (**3**), the second group contains 4-OCH_3−Ph- (**1**); 4-CH_3−Ph- (**4**); 4-CF_3−Ph- (**5**). Irrespective of the group and coordinates used, the same regularity is observed in the behavior of ΔG^{298}_{sub} functions and dimer structures. One can see a spread in values in both coordinates. First of all, it may be connected with the fact that the descriptors introduced are unable to describe specific interactions (coulomb, hydrogen bonding, and so on). Additional descriptors (multicorrelation equations) need to be introduced to take these interactions into consideration. It

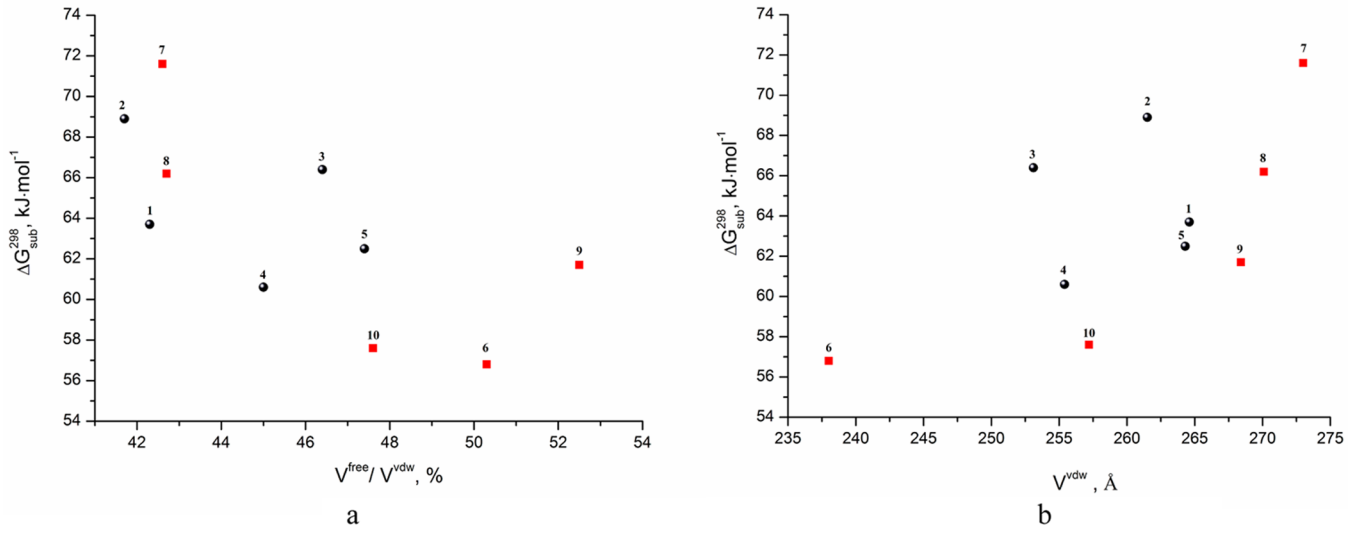

Figure 11. Plots of ΔG^{298}_{sub} versus V^{free}/V^{vdw} (a) and ΔG^{298}_{sub} versus V^{vdw} (b) for the compounds studied (red squares correspond to the crystals with dimers organization, black circles − with chains organization). Numbering corresponds to Figure 1.

dx.doi.org/10.1021/cg301511x | Cryst. Growth Des. XXXX, XXX, XXX−XXX

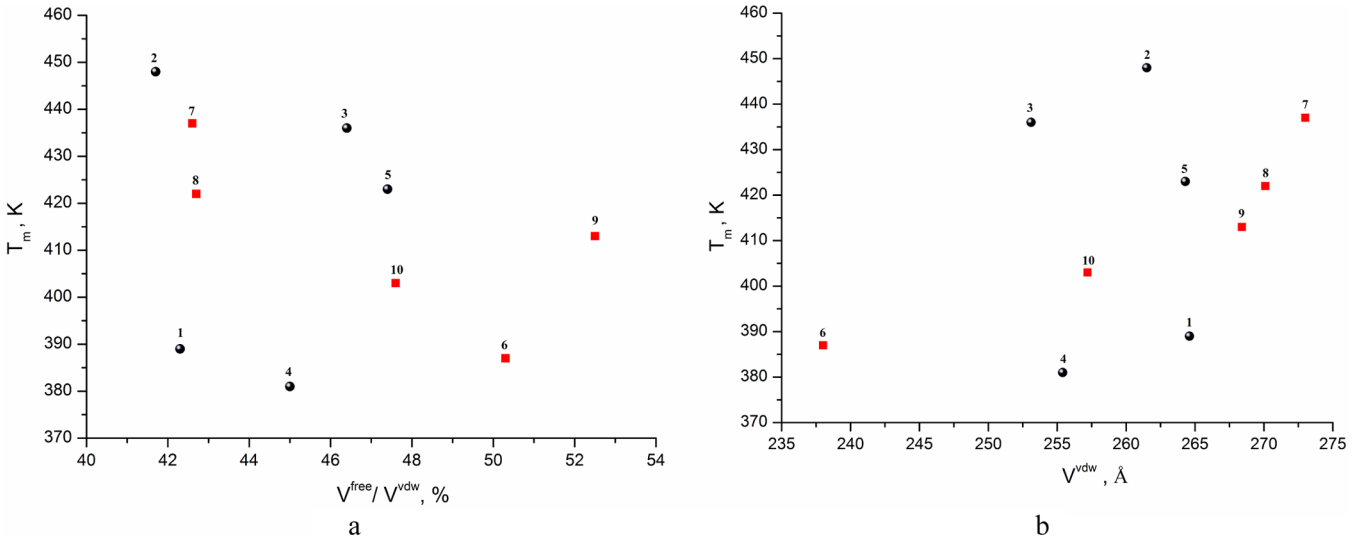

Figure 12. Plots of T_m versus V^{free}/V^{vdw} (a) and T_m versus V^{vdw} (b) for the compounds studied (red squares correspond to the crystals with dimers organization, black circles – with chains organization). Numbering corresponds to Figure 1.

seems to be impossible in our case due to the limited number of experimental points.

In pharmaceutics fusion temperature (T_m) is often applied as a parameter that indirectly specifies crystal lattice energy. It is due to the fact that thermophysical parameters (T_m, $\Delta H^{T_m}_{fus}$) can be easily obtained by routine DSC method. As an example, it is necessary to mention the general solubility equation (GSE) derived by Yalkowsky and Valvani,[28] which describes solubility of poorly soluble drug compounds in water. To illustrate how this parameter (T_m) is handled in pharmaceutics we tried to analyze the parameter by means of the above-mentioned β and V^{vdw} descriptors. The experimental T_m-values as functions of β (a) and V^{vdw} (b) are summarized in Figure 12a,b. It is not difficult to see that the discussed regularities match those observed for sublimation Gibbs energy (ΔG^{298}_{sub}). Thus, there should be some correlation between ΔG^{298}_{sub} and melting points. This relationship is especially evident in Figure 13: the increase in T_m makes Gibbs energy values to increase too. It should be noted that the branches of both dimer and chain crystal structures coincide in many respects. Only the values for methyl-phenyl- and methoxyphenyl- derivatives are much higher than all other values. It may be attributed to various mechanisms of participation of free volumes in sublimation and fusion processes.

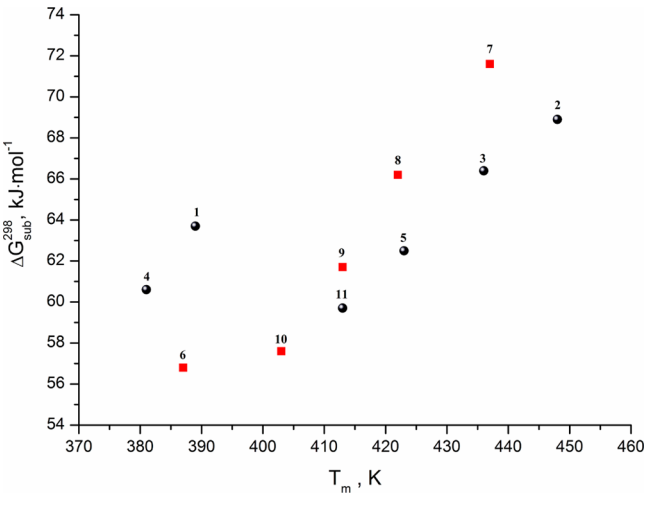

Figure 13. Relationship between the sublimation Gibbs energies (ΔG^{298}_{sub}) and melting points of the compounds studied (red squares correspond to the crystals with dimers organization, black circles – with chains organization). Numbering corresponds to Figure 1.

Contribution of Molecular Fragments to Crystal Packing Energy. One of the most interesting questions that arise during the analysis of crystal lattice architecture is the effect of various structural fragments of molecule on packing energy. In this context, we have developed an approach based on evaluation of nonbonded van der Waals interactions between different molecular fragments of adjacent molecules.[22,29] The concept may be useful enough to understand energetical aspects of crystal lattice formation beginning from nucleation processes up to bulk phase growth. Generally, structurally related molecules under investigation can be divided into several fragments, where one of these fragments remains unchanged while the others undergo some alterations. Algorithm of alteration may be arbitrary: (a) the increase in van der Waals volume at the expense of addition of chemically related groups; (b) gain in volume at the expense of adding chemically unlike groups; (c) conservation of the fragment volume and changing its topological structure, etc. In this context, van der Waals volume ratios of the fragments will change for (a) and (b) cases and influence the thermodynamic characteristics of a crystal lattice that, in turn, will define crystal packing architecture. In the case with (c) the volume of the molecule itself (and that of its fragments) remains constant, but conformations (and conformational stresses associated) change greatly thus contributing directly to crystal lattice architecture.

In the present work, the molecules under study were divided into two fragments (1 and 2) which are shown in Scheme 1. After that we calculated the contribution of nonbonded van der Waals interactions to the packing energy from different fragment pairs of adjacent molecules.

Use has been made of the two parameters as descriptors, namely, van der Waals and β parameter to analyze contributions of the fragments to crystal packing energy (we used the same parameters when studying thermodynamic characteristics of sublimation and fusion processes). The results

dx.doi.org/10.1021/cg301511x | Cryst. Growth Des. XXXX, XXX, XXX–XXX

Scheme 1

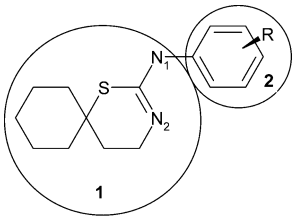

of the calculation for various energy terms of the studied crystal lattices are shown in Figure 14.

First, it follows from Figure 14 that contributions to packing energy may be arranged in the order: $E^{1-1} > E^{1-2} = E^{2-1} > E^{2-2}$. Second, the growth of β-parameter (the decrease in molecular packing density in a crystal) leads to an increase in the first fragments' contribution to packing energy. And finally, the growth of van der Waals volume of a molecule also causes an increase in contributions of the second fragments.

To assess the effect of a substituent on fragment interactions of comparable and overlapping terms, the following designations have been introduced: $\Delta E(11;22) = E^{1-1} - E^{2-2}$, $\Delta E(11;12) = E^{1-1} - E^{1-2}$ and $\Delta E(22;21) = E^{2-2} - E^{2-1}$. The results of the analysis are given in Figure 15. When van der Waals volume increases due to the growth in volume of the second fragment, the difference in contributions to crystal packing energy as a result of the interaction of the first and the second fragments $\Delta E(11;22)$ becomes less pronounced. Analogous tendency is observed for the difference in contributions between the second and overlapping fragments - $\Delta E(11;12)$. The proliferation of β value results in an equivalent increase in $\Delta E(11;22)$ and $\Delta E(11;12)$ values (Figure 15a). Unfortunately, no regularities are observed for $\Delta E(22;21)$.

CONCLUDING REMARKS

The crystal structures of 10 spiro-derivatives of 1,3-thiazine have been determined by X-ray diffraction. Molecular conformational states, packing architecture, and hydrogen bond networks have been studied by using graph set notations. According to topology of hydrogen bond network, all the compounds can be arbitrarily subdivided into two groups. The first group comprises compounds that form infinite chains of hydrogen bonds with four included atoms, $C_1^1(4)$, (five compounds; **1**−**5**), while the second one contains dimers forming rings with eight atoms, $R_2^2(8)$ (five compounds; **6**−**10**).

Analysis of dihedral ∠C11−S1−C8−N2 angles as a function of β parameter leads to following results. The angle remains practically invariable for compounds that form hydrogen bond networks in the form of infinite chains $C_1^1(4)$, whereas, for compounds forming dimers $R_2^2(8)$ the angle increases as molecule packing density in a crystal becomes smaller (proliferation of $\beta = V^{free}/V^{vdw}$ parameter).

Introducing any substituent in para- position of phenyl ring causes packing density in a crystal to increase (diminishing of β-parameter), the exception being 4-C_2H_5−Ph- substituent (**9**). As a result, molecular packing density becomes considerably smaller in comparison with the unsubstituted compound.

The sublimation thermodynamic aspects of the spiro-derivatives of 1,3-thiazine were studied by investigating the temperature dependence of vapor pressure using the transpiration method. Thermophysical study of fusion processes of the molecular crystals was carried out. It is observed that the increase in β-parameter results in lowering sublimation Gibbs energy for both dimers and chains crystal structures. Regularities of changing T_m as functions of β and V^{vdw} parameters are in agreement with those observed for ΔG_{sub}^{298}. There exists certain correlation between ΔG_{sub}^{298} and melting points. The proliferation of the latter is accompanied by the growth of Gibbs energy values. It should be noted that branches of dimers and chains crystal structures also coincide.

Contributions to the packing energy can be arranged in the following way: $E^{1-1} > E^{1-2} = E^{2-1} > E^{2-2}$. The contribution of the first group of fragments to the packing energy increases with the growth of β-parameter (diminishing of molecule packing density in a crystal). Contributions due to the second fragment interactions also gain in magnitude with the increase in molecular van der Waals volume. To assess the effect of a substituent on fragment interactions of comparable and overlapping terms, the following designations have been

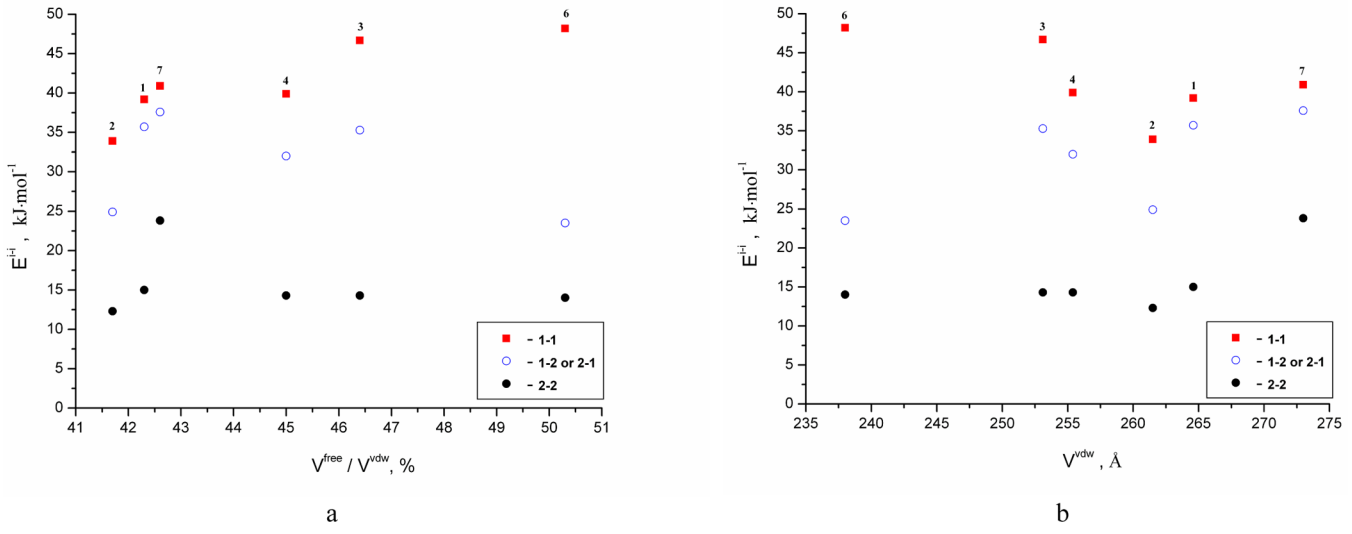

Figure 14. Relationship between the contributions from various molecular fragments in the packing energy made by the nonbounded van der Waals interactions (E^{i-i}) and V^{free}/V^{vdw} (a) and V^{vdw} (b). Numbering corresponds to Figure 1.

dx.doi.org/10.1021/cg301511x | Cryst. Growth Des. XXXX, XXX, XXX−XXX

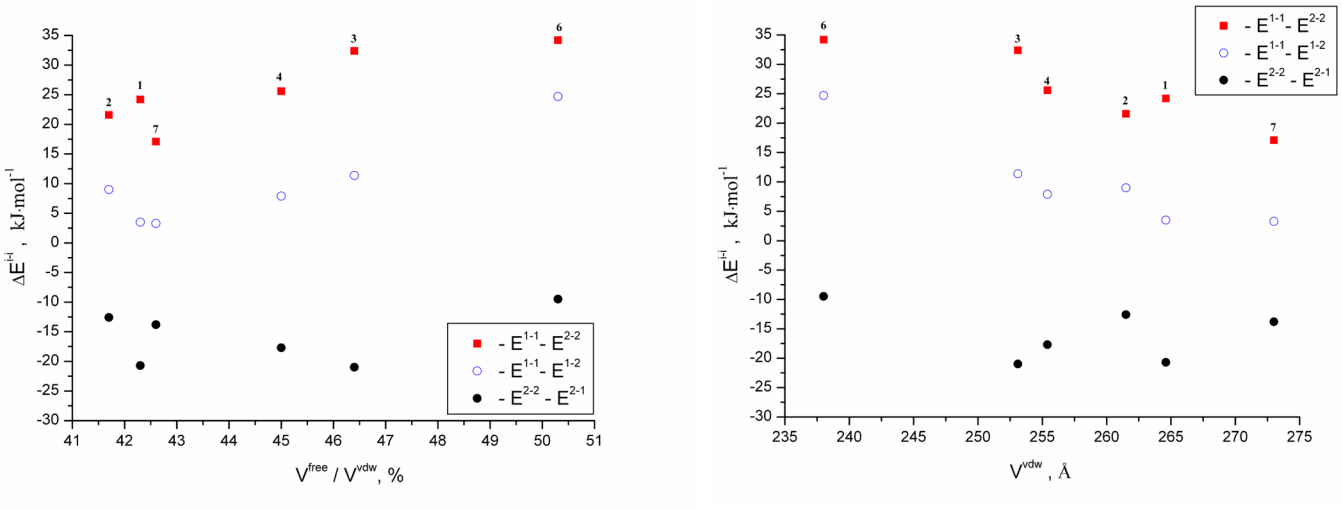

Figure 15. Relationship between ΔE^{i-i} and V^{free}/V^{vdw} (a) and between ΔE^{i-i} and V^{vdw} (b). Numbering corresponds to Figure 1.

introduced: $\Delta E(11;22) = E^{1-1} - E^{2-2}$, $\Delta E(11;12) = E^{1-1} - E^{1-2}$ and $\Delta E(22;21) = E^{2-2} - E^{2-1}$. When van der Waals volume increases due to the growth in volume of the second fragment, the difference in contributions to crystal packing energy as a result of the interaction of the first and the second fragments $\Delta E(11;22)$ becomes less pronounced. Analogous tendency is observed for the difference in contributions between the second and overlapping fragments - $\Delta E(11;12)$. The proliferation of β value results in an equivalent increase in $\Delta E(11;22)$ and $\Delta E(11;12)$ values.

■ ASSOCIATED CONTENT

Supporting Information

X-ray crystallographic information and additional figures. This material is available free of charge via the Internet at http://pubs.acs.org. The crystallographic data for **1**−**10** have been deposited with the Cambridge Crystallographic Data Centre, CCDC numbers 894490−894499. These data can be obtained free of charge from The Cambridge Crystallographic Data Centre via www.ccdc.cam.ac.uk/data_request/cif.

■ AUTHOR INFORMATION

Corresponding Author

*Telephone: +7-4932-533784. Fax: +7-4932-336237. E-mail glp@isc-ras.ru.

Notes

The authors declare no competing financial interest.

■ ACKNOWLEDGMENTS

This work was supported by the Federal Agency for Science and Innovations (N 02.740.11.0857) and the Russian Foundation of Basic Research N 12-03-00019.

■ REFERENCES

(1) Lipton, S. *Nat. Rev. Drug Discovery* **2006**, *5*, 2−11.
(2) Perlovich, G. L.; Proshin, A. N.; Volkova, T. V.; Kurkov, S. V.; Grigoriev, V. V.; Petrova, L. N.; Bachurin, S. O. *J. Med. Chem.* **2009**, *52*, 1845−1852.
(3) Amidon, G. L.; Lennernäs, H.; Shah, V. P.; Crison, J. R. *Pharm. Res.* **1995**, *12*, 413−420.
(4) Takagi, T.; Ramachandran, C.; Bermejo, M.; Yamashita, S.; Yu, L. X.; Amidon, G. L. *Mol. Pharmaceutics* **2006**, *3* (6), 631−643.
(5) Thayer, A. M. *Chem. Eng. News* **2010**, *88* (May 31), 13−18.
(6) Brittain, H. G. *J. Pharm. Sci.* **2007**, *96*, 705−728.
(7) Pudipeddi, M.; Serajuddin, A. T. M. *J. Pharm. Sci.* **2005**, *94*, 929−939.
(8) Griesser, U. J. The Importance of Solvates, in Hilfiker, R., Ed.; *Polymorphism: in the Pharmaceutical Industry*; Wiley: Germany, 2006; pp 211−233.
(9) Perlovich, G. L.; Bauer-Brandl, A. *Curr. Drug Delivery* **2004**, *1*, 213−226.
(10) Blokhina, S. V.; Ol'khovich, M. V.; Sharapova, A. V.; Proshin, A. N.; Perlovich, G. L. *J. Chem. Eng. Data* **2012**, DOI: dx.doi.org/10.1021/je300143a.
(11) *CAD-4 Software*, Version 5.0; Enraf-Nonius: Delft, The Netherlands, 1989.
(12) *SHELXL97 and SHELXS97*; Sheldrick, G. M. University of Göttingen: Germany, 1997.
(13) Zielenkiewicz, W.; Perlovich, G.; Wszelaka-Rylik, M. *J. Therm. Anal. Calorim.* **1999**, *57*, 225−234.
(14) Cox, J. D.; Pilcher, G. *Thermochemistry of Organic and Organometallic Compounds*; London: Academic Press. 1970.
(15) Chickos, J. S.; Acree, W. E., Jr. *J. Phys. Chem. Ref. Data.* **2002**, *31* (2), 537−698.
(16) Pascual-Ahuir, J. L.; Silla, E. *J. Comput. Chem.* **1990**, *11*, 1047.
(17) Gavezzotti, A.; Filippini, G. Chapter 3. Energetic aspects of crystal packing: Experiment and computer simulations. In Gavezzotti, A., Eds.; *Theoretical Aspects and Computer Modeling of the Molecular Solid State*; John Wiley & Sons: Chichester, 1997; pp 61− 97.
(18) Gavezzotti, A.; Filippini, G. *J. Am. Chem. Soc.* **1995**, *117*, 12299−12305.
(19) Gavezzotti, A. *J. Am. Chem. Soc.* **2000**, *122*, 10724−10725.
(20) Osborn, J. C.; York, P. *J. Mol. Struct.* **1999**, *474*, 43−47.
(21) Li, Z. J.; Ojala, W. H.; Grant, D. J. W. *J. Pharm. Sci.* **2001**, *90* (10), 1523−1539.
(22) Perlovich, G. L.; Ryzhakov, A. M.; Tkachev, V. V.; Hansen, L. Kr. *Cryst. Growth Des.* **2011**, *11* (4), 1067−1081.
(23) Kitaigorodsky, A. I. *The Molecular Crystals. M: Science* **1971**.
(24) Perlovich, G. L.; Proshin, A. N.; Volkova, T. V.; Cong, T. B.; Bachurin, S. O. *Mol. Pharmaceutics* **2011**, *8*, 1807−1820.
(25) Perlovich, G. L.; Volkova, T. V.; Proshin, A. N.; Sergeev, D. Yu.; Cong, T. B.; Petrova, L. N.; Bachurin, S. O. *J. Pharm. Sci.* **2010**, *99* (9), 3754−3768.
(26) Surov, A. O.; Terekhova, I. V.; Bauer-Brandl, A.; Perlovich, G. L. *Cryst. Growth Des.* **2009**, *9* (7), 3265−3272.
(27) Lebedev, Yu. A., Miroshnichenko, E. A. Thermochemistry vaporization of organic compounds. *Heats of Evaporation, Sublimation and Saturated Vapor Pressure*; M: Nauka, 1981; p 216.

(28) Yalkowsky, S. H.; Valvani, S. C. *J. Pharm. Sci.* **1980**, *69*, 912−922.
(29) Perlovich, G. L.; Rodionov, S. V.; Bauer-Brandl, A. *Eur. J. Pharm. Sci.* **2005**, *24*, 25−33.
(30) Mayo, S. L.; Olafson, B. D.; Goddard, W. A., III *J. Phys. Chem.* **1990**, *94*, 8897−8909.